Earth Surf. Dynam., 3, 441–445, 2015
www.earth-surf-dynam.net/3/441/2015/
doi:10.5194/esurf-3-441-2015

Earth Surface Dynamics
Open Access

Short Communication: Evidence for non-Gaussian distribution of rock weathering rates

S. Emmanuel

Institute of Earth Sciences, The Hebrew University of Jerusalem, Edmond J. Safra Campus, Givat Ram, Jerusalem, 91904, Israel

Correspondence to: S. Emmanuel (simonem@cc.huji.ac.il)

Received: 21 May 2015 – Published in Earth Surf. Dynam. Discuss.: 7 July 2015
Revised: 26 August 2015 – Accepted: 27 August 2015 – Published: 1 September 2015

Abstract. The weathering of rocks influences the geochemistry of the oceans, the erosion of landscapes and man-made structures, and even the global climate. Although a high degree of variance is often observed in rate measurements, little is understood about the statistical characteristics of weathering rate distributions. This preliminary study demonstrates that the weathering rates of limestone, determined from measurements of an ancient eroded limestone edifice, can exhibit highly non-Gaussian behavior. While a Gaussian model produced a poor fit with the data, an alternative model – the generalized extreme value (GEV) framework – was capable of capturing the asymmetric long-tailed distribution, in good agreement with the measured curve. Furthermore, the non-Gaussian distribution of these field rates was found to have similar characteristics to the distribution of rates measured over much smaller microscopic regions of limestone surfaces in laboratory experiments. Such similar behavior could be indicative of analogous chemical and mechanical weathering processes acting over a range of spatial and temporal scales. Moreover, highly asymmetric rate distributions with high variance could be characteristic of rates not only in carbonate rocks, but also in other rock types, suggesting that the use of a small number of measurements to determine field weathering rates may be insufficient to fully characterize the range of rates in natural systems.

1 Introduction

Rock weathering is a ubiquitous process that influences the erosion of buildings and monuments, the evolution of landscapes, and the geochemical balance of the oceans (Liu and Zhao, 2000; Basak and Martin, 2013; Komar et al., 2013). Moreover, weathering also plays a role in mediating CO_2 levels in the atmosphere (e.g., Berner and Kothavala, 2001), potentially affecting climate not only on geological timescales but also on shorter timescales of hundreds to thousands of years (Liu et al., 2011). Despite its significance, measuring the rates of rock weathering has proved a challenging task, sometimes yielding rates that vary significantly (White and Brantley, 2003), even at closely related outcrops (e.g., Ryb et al., 2014a, b). While such variability may be partly due to the analytical uncertainty inherent in some of the methods used, it is also likely to reflect the natural heterogeneity governing weathering processes in field settings (Navarre-Sitchler and Brantley, 2007), making it difficult to isolate the controlling mechanisms. In the case of carbonate rock weathering, although the amount of precipitation plays a dominant role in determining weathering rates, a high degree of variance is typical of field measurements (Fig. 1).

Recent characterization of carbonate rock reaction rates at the micron and nanometer scale suggests that the distribution of reaction rates can be highly non-Gaussian (Fischer et al., 2012), and this is likely to reflect the combination of different modes of surface retreat (Schott et al., 1989; Luttge et al., 2013), such as rapid reaction along grain boundaries, slow dissolution at crystal faces, and even the mechanical detachment of micron-scale grains (Emmanuel, 2014; Emmanuel and Levenson, 2014). Using a similar approach, detailed characterization of the rate distributions at the outcrop level could provide crucial information concerning the factors – such as mineralogical heterogeneity and textural features – that potentially control weathering at larger spatial

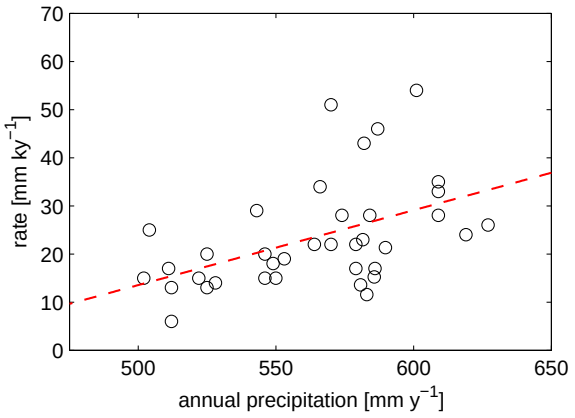

Figure 1. Limestone weathering rates for a restricted range of annual precipitation in the eastern Mediterranean. Although precipitation is thought to be the dominating factor, the variance for any given level of precipitation is large, with values deviating from the least-squares fit line by over 100 %. Data compiled from Ryb et al. (2014a) and Ryb et al. (2014b).

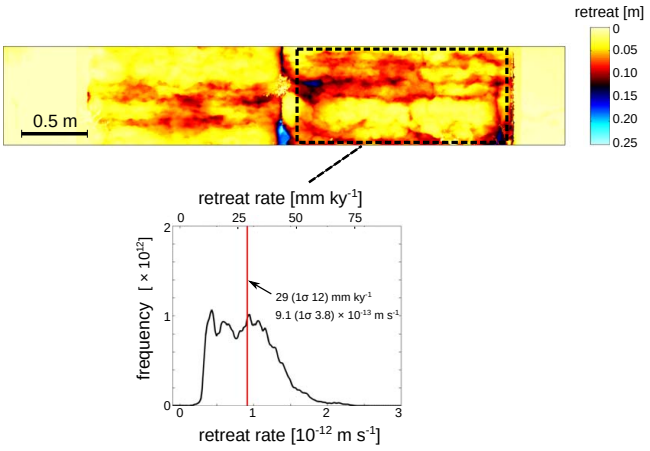

Figure 2. Surface retreat map and associated retreat rate spectrum for a section of the Western Wall. The retreat rate is calculated relative to a false datum reconstructed from well-preserved blocks flanking the eroded region. Data from Emmanuel and Levenson (2014).

scales. At present, however, most field-based measurements of weathering rates employ geochemical methods, which yield too few values to carry out a comprehensive statistical analysis of spatial variability. Here, an alternative approach is taken, involving the analysis of a lidar scan of an ancient limestone edifice. To shed light on the statistical characterization of weathering rates, the shape of the rate distribution is explored, and a theoretical framework is used to describe the probability density functions for weathering rates. The results of the analysis are compared with laboratory experiments, and the implications for rock weathering rates at different scales are discussed.

2 Methods

2.1 Field data set and analysis

The field data set analyzed here was published previously in a study that explored the long-term weathering rates of limestone at the 2000-year-old Western Wall in Jerusalem (Emmanuel and Levenson, 2014). In that study, a high-resolution lidar scan was performed on the wall in 2010 using a Surphaser 25HSX (rated noise range of 0.2 mm at a working distance of 8 m). Retreat rates were estimated by selecting blocks that (i) had no obvious signs of anthropogenic damage and (ii) were flanked by well-preserved stones on either side within the same course. A plane fitting algorithm was applied to points on each of the flanking blocks, thereby creating a false datum which could be used to estimate the degree of surface retreat (Fig. 2). This technique provided a large number of data points ($\sim 28\,000$ points m^{-2}) which were used to calculate the probability density functions of weathering rates – or rate spectra (Fischer et al., 2012; Luttge et al., 2013; Emmanuel, 2014) – using the kernel density estimation method (Vermeesch, 2012). Here, data from four individual, meter-scale blocks were compiled to produce a single area-weighted rate spectrum for weathering. Using this method, uncertainties are estimated to be ± 1 mm ky^{-1}. The highly eroded blocks all comprise calcareous micritic limestone, containing bedding parallel stylolites, from the Netzer Formation. By contrast, the more resistant flanking blocks were hewn from much coarser calcareous grain stone from the Shivta Formation, with a representative grain size of approximately 50 µm.

As the probability density functions associated with weathering rates often exhibit a high degree of asymmetry, a flexible model that is capable of capturing a wide range of behaviors is required. One framework that provides a high level of flexibility is extreme value theory, which has been used to analyze the frequency of rare events, such as extreme weather phenomena (Nadarajah, 2005), flooding (Chowdhury et al., 1991; Nadarajah and Shiau, 2005), and earthquakes (Burton and Makropoulos, 1985; Osella et al., 1992). In addition, it has also been shown that extreme value theory is effective at describing the evolution of corrosion pits on metal surfaces (e.g., Scarf et al., 1992), and at reproducing the highly asymmetric long tails in the rate spectra of reaction rates of dissolving dolostone surfaces (Emmanuel, 2014).

The generalized extreme value (GEV) frequency distribution function, P_{GEV}, has the following mathematical form (Kotz and Nadarajah, 2000):

$$P_{\mathrm{GEV}} = \frac{1}{\sigma} t(r)^{\xi+1} \exp\left(-t(r)\right), \tag{1}$$

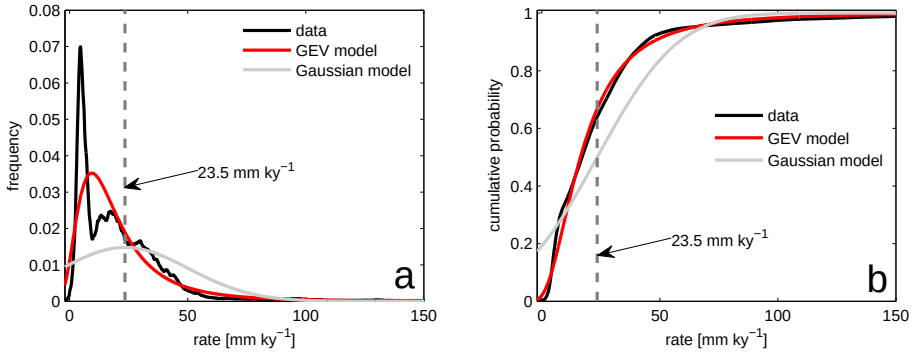

Figure 3. **(a)** Retreat rate spectrum based on a compilation of four eroded micritic limestone blocks at the Western Wall. Best fits for generalized extreme value (GEV) and Gaussian models are shown. The fitting parameters for the GEV model are $\mu = 12.1\,\mathrm{mm\,ky^{-1}}$, $\sigma = 10.9\,\mathrm{mm\,ky^{-1}}$, and $\xi = 0.296$; parameters for the Gaussian model are $\mu_g = 23.5\,\mathrm{mm\,ky^{-1}}$ and $\sigma_g = 27.0\,\mathrm{mm\,ky^{-1}}$. **(b)** Cumulative distribution functions for the weathering rates shown together with the GEV and Gaussian models.

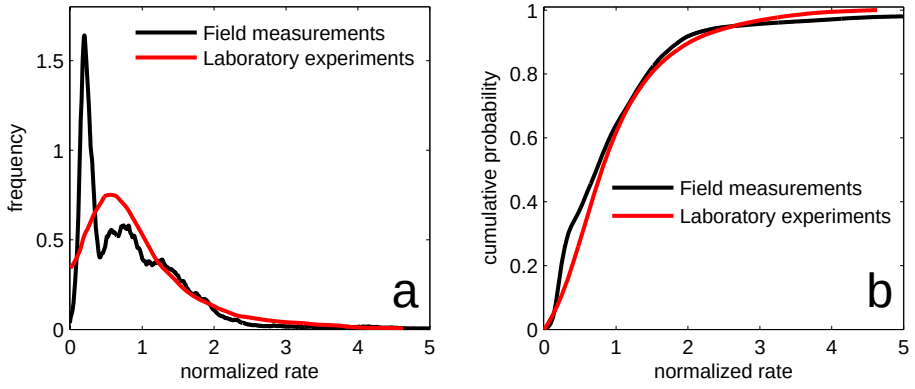

Figure 4. **(a)** Spectra of weathering rates of micritic limestone derived from field measurements and rates determined in laboratory experiments reported by Fischer et al. (2012). For each curve, the rates have been normalized to the mean rate in each data set. **(b)** Cumulative distribution functions for the two data sets.

where

$$t(r) = \begin{cases} \left(1 + \left(\dfrac{r-\mu}{\sigma}\right)\xi\right)^{-1/\xi} & \text{if } \xi \neq 0, \\ \exp\left(-\dfrac{(r-\mu)}{\sigma}\right) & \text{if } \xi = 0. \end{cases} \quad (2)$$

In these equations, r is the rate, σ is the scale parameter, ξ is the shape parameter, and μ is the location parameter. Using a built-in Matlab fitting function, optimal model parameters were obtained for the rate spectrum. For comparison, the measured distribution was also fitted with a Gaussian model:

$$P_{\mathrm{GAUSS}} = \frac{1}{\sigma_g\sqrt{2\pi}} \exp\left(-\frac{(r-\mu_g)^2}{2\sigma_g^2}\right), \quad (3)$$

where σ_g is the standard deviation and μ_g is the mean value.

3 Results and discussion

The rate spectrum of the compiled Western Wall data set exhibits a highly asymmetric distribution (Fig. 3), with a prominent peak at approximately $4.6\,\mathrm{mm\,ky^{-1}}$, a mean of $23.5\,\mathrm{mm\,ky^{-1}}$, and a long tail that extends to $> 100\,\mathrm{mm\,ky^{-1}}$. Importantly, the Gaussian model is unable to produce a satisfactory fit, missing both the peak rates and the long tail in the data. By contrast, the generalized extreme value model matches the data set with much greater fidelity, both in terms of capturing the peak value and the long tailing. Thus, the analysis indicates that the rates in the compiled data set exhibit significantly non-Gaussian characteristics.

Significantly, such non-Gaussian behavior in rock weathering is not restricted to the field scale. In laboratory experiments that employed vertical scanning interferometry to observe the retreat rates of a reacting micritic limestone (fossil-free Triassic Muschelkalk from Germany) over regions approximately $50\,\mu\mathrm{m} \times 50\,\mu\mathrm{m}$ in size, Fischer et al. (2012) reported similar asymmetric, long-tailed distributions. When the surface retreat rates are normalized to the average value in each data set, a comparison of the field-derived rates with the laboratory-measured rates reveals remarkably similar behavior (Fig. 4). The similarity between the patterns is espe-

cially surprising given that the length scales of observation in the two data sets differ by more than 4 orders of magnitude (tens of microns in the laboratory experiments versus meters in the field), while the temporal scales are separated by 6 orders of magnitude (hours versus thousands of years). Moreover, while the studied rocks in both cases are micritic limestone, they are from completely different geological formations and geographical locations.

The non-Gaussian distributions observed in both the field measurements and laboratory experiments could be indicative of the overall similarity of processes controlling the evolution of weathering surfaces at different spatial scales. Recently, Emmanuel and Levenson (2014) suggested that the potential chemical weathering rate at the Western Wall site was too low to account for the measured average rate, and that mechanical weathering is likely to have made a significant contribution to erosion. In that same study, atomic force microscopy was used to observe the reaction of micritic limestone in water, and it was found that dissolution along micron-scale grain boundaries was often followed by the detachment of tiny grains. This chemo-mechanical process was suggested to be one of the mechanisms accelerating weathering in limestones at larger scales. However, additional textural and structural features – including stylolites, joints, and fractures – which appear at a range of different scales, could facilitate the detachment of larger particles, ultimately controlling the evolution of rock surfaces at greater spatial scales. In fact, visual inspection of the Western Wall reveals that highly eroded regions are often associated with stylolite surfaces (Fig. 5a), and the tiny gaps that can be observed between the seams are consistent with the detachment of small particles (Fig. 5b). High-resolution laboratory experiments demonstrate that micron-scale grain detachment in carbonate rocks produces rate spectra that are highly asymmetric and non-Gaussian (Emmanuel, 2014), and the stochastic mechanical removal of millimeter and centimeter size particles could also produce a similar distribution of weathering patterns at the outcrop scale. Crucially, if the processes controlling patterns at the meter scale are indeed analogous to those acting at the micron scale, high-resolution experiments might provide a way to gain insight into the much slower, large-scale processes controlling erosional patterns in the field. However, caution must clearly be taken when interpreting field patterns because additional mechanisms – such as bio-mechanical weathering mediated by plants, lichens, and even microbes – could potentially produce similar non-Gaussian patterns.

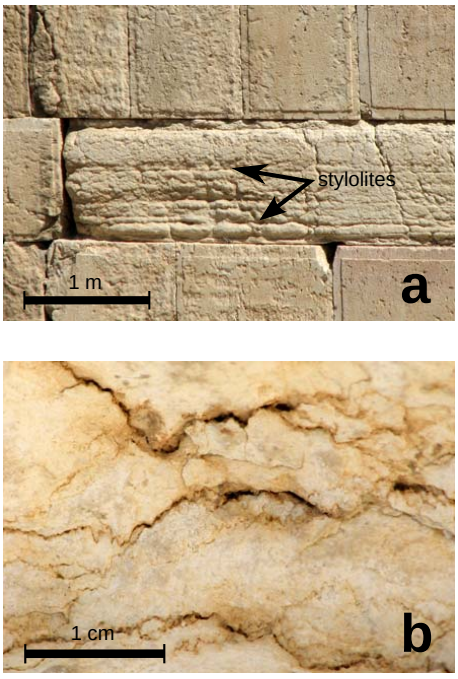

Figure 5. **(a)** A section of the Western Wall showing enhanced weathering in a block of micritic limestone containing stylolites. **(b)** Close-up of a limestone block with stylolites. The millimeter-scale gaps between the seams may be indicative of mechanical particle detachment.

4 Conclusions

In this study, the weathering rates of carbonate rocks for a long-term field data set were found to have highly non-Gaussian characteristics. In contrast to the Gaussian model, the generalized extreme value (GEV) framework was capable of capturing the long-tailed distributions, producing good fits with the measured curves. Furthermore, the non-Gaussian distribution was found to be similar to that reported for laboratory experiments examining microscopic regions of limestone surfaces. Such similar behavior could be indicative of analogous chemical and mechanical weathering processes acting over a range of different spatial and temporal scales.

While the GEV model performs well at characterizing the statistics of weathering rates, the brief analysis presented here clearly has limitations. In this study, due to a lack of suitable data, only two data sets, examining one type of lithology, were analyzed. As a result, precisely how widespread non-Gaussian weathering distributions are remains unclear, and whether similar patterns will also be observed in other lithologies – such as silicate rocks, which weather much more slowly – has also yet to be determined. Moreover, on a mechanistic level, although the asymmetry of the rate distributions is a product of the various chemical, physical, and biological processes shaping the eroding rock surfaces, it is still uncertain precisely which mechanisms dominate which regions of the rate spectra. Resolving these issues, however, requires the collection and characterization of rate spectra from additional field data sets, ideally using time-lapse methods, as well as laboratory studies that examine a range of different rock types.

Despite the limitations identified above, this preliminary analysis has a number of important implications for weathering studies. Firstly, the potentially high variance in both field and laboratory rates means that extreme care must be taken when interpreting a limited number of rate measurements. In field studies that employ geochemical methods, such as cosmogenic radionuclide dating, this problem may be particularly acute as only a handful of samples are often relied upon to determine weathering rates. Secondly, the similarity between the behavior of field and laboratory rates suggests that there may be a way to bridge observations at very different scales. It is often noted that the weathering rates determined in field studies are usually much slower than those measured under laboratory conditions, and the source of this discrepancy is hotly debated (e.g., Swoboda-Colberg and Drever, 1993; White and Brantley, 2003; Ganor et al., 2007; Emmanuel and Ague, 2011). It may be the case that at least some of the observed disparity could be due to scale-dependent processes, and examining rate distributions across different scales, and in different lithologies, could provide an improved mechanistic understanding that would help resolve this issue.

Acknowledgements. S. Emmanuel thanks the Israel Science Foundation for their generous support. Robert Inkpen, Alexis Navarre-Sitchler, and Heather Viles are thanked for their helpful comments.

Edited by: H. Viles

References

Basak, C. and Martin, E. E.: Antarctic weathering and carbonate compensation at the Eocene-Oligocene transition, Nat. Geosci., 6, 121–124, 2013.

Berner, R. A. and Kothavala, Z.: GEOCARB III: a revised model of atmospheric CO_2 over Phanerozoic time, Am. J. Sci., 301, 182–204, 2001.

Burton, P. W. and Makropoulos, K. C.: Seismic risk of circum Pacific earthquakes: II. Extreme values using Gumbel's third distribution and the relationship with strain energy release, Pure Appl. Geophys., 123, 849–866, 1985.

Chowdhury, J., Stedinger, J., and Lu, L.: Goodness-of-fit tests for regional generalized extreme value flood distributions, Water Resour. Res., 27, 1765–1776, 1991.

Emmanuel, S.: Mechanisms influencing micron and nanometer-scale reaction rate patterns during dolostone dissolution, Chem. Geol., 363, 262–269, 2014.

Emmanuel, S. and Ague, J. J.: Impact of nano-size weathering products on the dissolution rates of primary minerals, Chem. Geol., 282, 11–18, 2011.

Emmanuel, S. and Levenson, Y.: Limestone weathering rates accelerated by micron-scale grain detachment, Geology, 42, 751–754, 2014.

Fischer, C., Arvidson, R. S., and Lüttge, A.: How predictable are dissolution rates of crystalline material?, Geochim. Cosmochim. Ac., 98, 177–185, 2012.

Ganor, J., Lu, P., Zheng, Z., and Zhu, C.: Bridging the gap between laboratory measurements and field estimations of silicate weathering using simple calculations, Environ. Geol., 53, 599–610, 2007.

Komar, N., Zeebe, R., and Dickens, G.: Understanding long-term carbon cycle trends: The late Paleocene through the early Eocene, Paleoceanography, 28, 650–662, 2013.

Kotz, S. and Nadarajah, S.: Extreme Value Distributions: Theory and Applications, Imperial College Press, London, 2000.

Liu, Z., Dreybrodt, W., and Liu, H.: Atmospheric CO_2 sink: Silicate weathering or carbonate weathering?, Appl. Geochem., 26, S292–S294, 2011.

Liu, Z.-h. and Zhao, J.: Contribution of carbonate rock weathering to the atmospheric CO_2 sink, Environ. Geol., 39, 1053–1058, 2000.

Luttge, A., Arvidson, R. S., and Fischer, C.: The mineral water interface: a stochastic treatment of crystal dissolution kinetics, Elements, 9, 183–188, 2013.

Nadarajah, S.: Extremes of daily rainfall in west central Florida, Climatic Change, 69, 325–342, 2005.

Nadarajah, S. and Shiau, J.: Analysis of extreme flood events for the Pachang River, Taiwan, Water Resour. Manag., 19, 363–374, 2005.

Navarre-Sitchler, A. and Brantley, S.: Basalt weathering across scales, Earth Planet. Sc. Lett., 261, 321–334, 2007.

Osella, A. M., Sabbione, N. C., and Cernadas, D. C.: Statistical-analysis of seismic data from North-Western and Western Argentina, Pure Appl. Geophys., 139, 277–292, 1992.

Ryb, U., Matmon, A., Erel, Y., Haviv, I., Katz, A., Starinsky, A., Angert, A., and ASTER Team: Controls on denudation rates in tectonically stable Mediterranean carbonate terrain, Geol. Soc. Am. Bull., 126, 553–568, 2014a.

Ryb, U., Matmon, A., Erel, Y., Haviv, I., Katz, A., Benedetti, L., and Hidy, A. J.: Styles and rates of long-term denudation in carbonate terrains under a Mediterranean to hyper-arid climatic gradient, Earth Planet. Sc. Lett., 406, 142–152, 2014b.

Scarf, C. R., Cottis, R. A., and Laycock, P.: Extrapolation of extreme pit depths in space and time using the r-deepest pit depths, J. Electrochem. Soc., 139, 2621–2627, 1992.

Schott, J., Brantley, S., Crerar, D., Christophe, G., Borcsik, M., and Willaime, C.: Dissolution kinetics of strained calcite, Geochim. Cosmochim. Ac., 53, 373–382, 1989.

Swoboda-Colberg, N. G. and Drever, J. I.: Mineral dissolution rates in plot-scale field and laboratory experiments, Chem. Geol., 105, 51–69, 1993.

Vermeesch, P.: On the visualisation of detrital age distributions, Chem. Geol., 312–313, 190–194, 2012.

White, A. F. and Brantley, S. L.: The effect of time on the weathering of silicate minerals: Why do weathering rates differ in the laboratory and field?, Chem. Geol., 202, 479–506, 2003.